Delay- and Coupling-Induced Firing Patterns in Oscillatory Neural Loops

Oleksandr V. Popovych,[1] Serhiy Yanchuk,[2] and Peter A. Tass[1,3]
[1]*Institute of Neuroscience and Medicine-Neuromodulation (INM-7), Research Center Jülich, 52425 Jülich, Germany*
[2]*Institute of Mathematics, Humboldt University of Berlin, 10099 Berlin, Germany*
[3]*Department of Stereotaxic and Functional Neurosurgery, University Hospital, 50924 Cologne, Germany*

(Received 15 July 2011; published 21 November 2011)

For a feedforward loop of oscillatory Hodgkin-Huxley neurons interacting via excitatory chemical synapses, we show that a great variety of spatiotemporal periodic firing patterns can be encoded by properly chosen communication delays and synaptic weights, which contributes to the concept of temporal coding by spikes. These patterns can be obtained by a modulation of the multiple coexisting stable in-phase synchronized states or traveling waves propagating along or against the direction of coupling. We derive explicit conditions for the network parameters allowing us to achieve a desired pattern. Interestingly, whereas the delays directly affect the time differences between spikes of interacting neurons, the synaptic weights control the phase differences. Our results show that already such a simple neural circuit may unfold an impressive spike coding capability.

DOI: 10.1103/PhysRevLett.107.228102 PACS numbers: 87.19.lj, 05.45.Xt, 87.19.lp

According to the temporal coding hypothesis the information in the neural spike train emitted by a single neuron or by a neural population is carried by the timing of action potentials [1]. A neural population must thus be able to produce a variety of spatiotemporal firing patterns in order to form dynamical cell assemblies, which are hypothesized to be crucial for information processing, transfer, and storage [2]. The proper formation of such assemblies requires a precise constellation of firing times of neurons, latencies of signal propagation, and the coupling topology, enabling a fine coordination of firing patterns and their reliable detection [3]. It is thus important to understand how the modulation of signal propagation delays and synaptic weights can affect the formation of spatiotemporal firing patterns.

The brain is a highly adaptive structure since the synaptic weights can permanently be adjusted due to the spike timing-dependent plasticity (STDP); see review [4]. Propagation delays seem to be well tuned in the brain [5] and can be adapted either by synaptic selection (e.g., by STDP) out of a spectrum of many possible delay lines [6] or directly by changing length and thickness of dendrites and axons, the extent of myelination of axons, variation of synaptic latencies, etc. [7]. Accordingly, pathological alterations of the signal conductance can severely impair neural information processing as, for example, in the case of axon demyelination in multiple sclerosis [8].

In this Letter we explicitly show how a multitude of firing patterns emerges and gets stored in an oscillatory neural loop by appropriate adjustment of communication delays and synaptic weights. On the one hand, delayed interactions can cause a time shift between signals, as experimentally demonstrated, e.g., in two lasers coupled with time delay [9]. On the other hand, delays can be compensated for, so that in-phase synchronization is still possible, as demonstrated in many delay-coupled networks [10,11]. The interest in the mechanisms giving rise to more complex spatiotemporal structures is increasing. A variety of spatiotemporal structures have been demonstrated for different coupling topologies for networks of integrate-and-fire-like neurons [12]; see also Ref. [13] for localized patterns and Ref. [14] for stabilization of neuronal bumps. Here we show that, more generally, for networks of generic limit-cycle (LC) oscillators and Hodgkin-Huxley (HH) spiking neurons coupled via excitatory chemical synapses, a strikingly broad spectrum of spatiotemporal firing patterns can be created and explicitly controlled by properly adjusting conductance delays and synaptic weights. For this we study networks of oscillators unidirectionally coupled in a ring [Fig. 1(a)]. Unidirectionally coupled loops are generic components in the nervous system [15] as intensively studied, e.g., in the context of pathological neural dynamics and deep brain stimulation [16]. The ring topology naturally appears in the context of excitable cardiac tissue and orientation tuning in visual cortex [17].

Obviously, our model is minimal with respect to the number of coupling edges, since only N connections exist in a network of N oscillators. On the one hand, this supports a unique representation of the firing patterns by coupling delays and coupling strengths. On the other hand, one might intuitively anticipate that the minimal topology of the unidirectionally coupled loop [Fig. 1(a)] might impose relevant restrictions on the type of emerging spatiotemporal firing patterns. We here, however, show that already such a comparably simple neural circuit might act as a coding machine that is able to produce a multitude of spatiotemporal firing patterns.

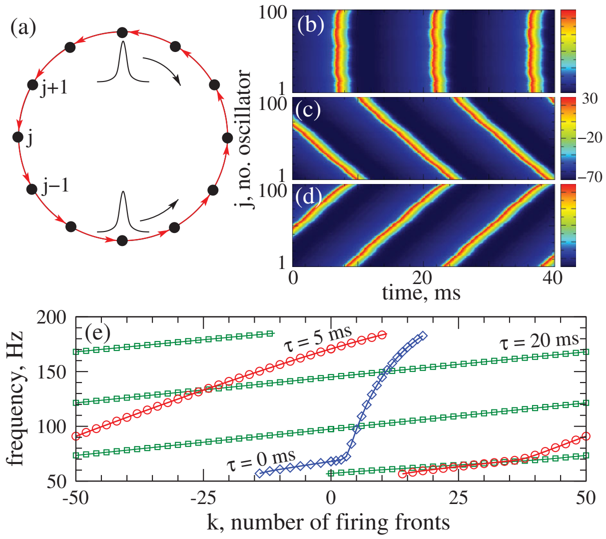

FIG. 1 (color). (a) Ring of unidirectionally coupled neurons. (b)–(d) Typical periodic spatiotemporal patterns appearing in homogeneously coupled (identical synaptic weights and communication delays) HH spiking neurons (1): (b) in-phase synchronization, (c),(d) traveling waves with one firing front propagating along ($k = 1$) and against ($k = -1$) the direction of coupling, respectively, see (a). Membrane potential V_j is encoded in color versus time and oscillator number. (e) Coexistence of multiple stable traveling waves, where the spiking frequency of synchronized neurons is depicted versus the number of firing fronts k for different identical delay τ in coupling and for initial vector functions $\Gamma(t)$, $t \in [-\tau, 0]$ with components $\Gamma_j(t) = \gamma(t + jTk/N)$, where $\gamma(t)$ approximates the waveform of the limit cycle of a neuron in the network, and T is its period. Parameters $C = 1\ \mu\mathrm{F/cm}^2$, $V_{Na} = 50$ mV, $V_K = -77$ mV, $V_l = -54.4$ mV, $g_{Na} = 120\ \mathrm{mS/cm}^2$, $g_K = 36\ \mathrm{mS/cm}^2$, and $g_l = 0.3\ \mathrm{mS/cm}^2$. The constant currents I_j are Gaussian distributed with mean 10 $\mu\mathrm{A/cm}^2$ and standard deviation 0.01. Delay $\tau_j = 0$ ms in (b)–(d), number of neurons $N = 100$, and coupling $K_j = 5\ \mathrm{mS/cm}^2$.

We consider periodically spiking HH neurons [18]

$$\begin{aligned}
C\dot{V}_j &= I_j - g_{Na} m_j^3 h_j (V_j - V_{Na}) - g_K n_j^4 (V_j - V_K) \\
&\quad - g_l (V_j - V_l) - K_j (V_j - V_r) s_{j+1}(t - \tau_j), \\
\dot{m}_j &= \alpha_m(V_j)(1 - m_j) - \beta_m(V_j) m_j, \\
\dot{h}_j &= \alpha_h(V_j)(1 - h_j) - \beta_h(V_j) h_j, \qquad (1) \\
\dot{n}_j &= \alpha_n(V_j)(1 - n_j) - \beta_n(V_j) n_j, \\
\dot{s}_j &= 5(1 - s_j)/\{1 + \exp[-(V_j + 3)/8]\} - s_j,
\end{aligned}$$

where the variable V_j, $j = 1, \ldots, N$, models the membrane potential of neuron j, and $\alpha_m(V) = (0.1V + 4)/[1 - \exp(-0.1V - 4)]$, $\beta_m(V) = 4\exp[(-V - 65)/18]$, $\alpha_h(V) = 0.07\exp[(-V - 65)/20]$, $\beta_h(V) = 1/[1 + \exp(-0.1V - 3.5)]$, $\alpha_n(V) = (0.01V + 0.55)/[1 - \exp(-0.1V - 5.5)]$, and $\beta_n(V) = 0.125\exp[(-V - 65)/80]$. The neurons are excitatory coupled (the reverse potential $V_r = 0$ mV) via the postsynaptic potentials s_j [19] in a ring such that $s_{N+1} \equiv s_1$ [Fig. 1(a)]. Parameter K_j defines the coupling strength, and τ_j is the time delay in the coupling.

In the existing literature on *homogeneous* ring-coupled systems, i.e., with parameters and couplings being all identical, typical spatiotemporal patterns have been revealed; see, e.g., [10,20]. Often, multiple coexisting stable traveling waves emerge or can be stabilized by feedback control methods [21], which turned out to be a typical form of activity propagation in the nervous system [22]. As a particular case, in-phase synchronized patterns are possible and can be stable. Such a dynamics can also be found for the HH neurons (1), where, depending on the initial conditions, the neurons can synchronize and fire either simultaneously [Fig. 1(b)] or with the time shift $t_j - t_{j+1} \approx Tk/N$ between the neighboring neurons. Here T is the period of oscillations. In the latter case, k firing fronts propagate along the network either in the direction of coupling [Fig. 1(c) for $k = 1$] or in the opposite direction [Fig. 1(d) for $k = -1$]. Although a single HH neuron exhibits a monostable periodic firing at the frequency $f \approx 68$ Hz for the considered parameters, the network demonstrates a great multistability of synchronized dynamics, which is significantly enhanced if a delay in coupling is introduced [Fig. 1(e)]. The coupled neurons can synchronize at a frequency ranging from 56 to 185 Hz and in numerous coexisting traveling waves. The neuronal dynamics within the synchronization manifolds of the above regular patterns for homogeneous loops of identical neurons (1) can be modeled by a single HH neuron with delayed self-feedback [23], where a delay-induced multistability has been found. However, in the case when the coupling strengths or delays are not identical, more complicated structures emerge, which are essentially network objects. To illustrate this phenomenon, we use the above simple patterns as reference patterns and then adjust time delays and synaptic weights to create a new desired pattern.

Delay-induced firing patterns.—Let a general network with identical delays $\dot{x}_j(t) = g_j(x_j(t), x_{j+1}(t - \tau))$ exhibit a stable reference pattern where the neurons fire at times $\{t_j\}_{j=1}^N$. Then the change of variables $y_j(t) = x_j(t - \eta_j)$ transforms the system to $\dot{y}_j(t) = g_j(y_j(t), y_{j+1}(t - \tau_j))$, where the delays $\tau_j = \tau - \eta_{j+1} + \eta_j$ are no longer identical, and the neurons fire at times $\{t_j + \eta_j\}_{j=1}^N$ up to some common shift. Thus, by choosing the delays appropriately, one can generate an arbitrary spiking pattern. Because of the translational invariance of the unidirectionally coupled system, the stability of a pattern is not affected as long as the total delay in the ring is kept constant. Nevertheless, the above arguments can be applied to other coupled systems with different coupling type and topology. A single limitation of this approach is that the time offset $\eta_{j+1} - \eta_j$ must be smaller than τ in order that all delays τ_j will be positive. This bounds the width of the spike patterns and underlines the importance of a positive delay τ in the coupling.

The above delay-induced patterns can be applied to any stable synchronized dynamics of HH neurons (1) [Figs. 1(b)–1(e)]. We illustrate this by a random pattern (the spiking times η_j are uniformly distributed in the interval $[-3, 3]$ ms) modulating the in-phase synchronized reference pattern [Fig. 2(a)] and by a pattern resembling the abbreviation "PRL" and modulating a traveling wave reference pattern with $k = -1$ firing fronts [Fig. 2(c)]. The filled red diamonds in Figs. 2(a) and 2(c) depict the theoretically predicted patterns $\{\eta_j - jTk/N\}$ and perfectly fit the numerical simulations. The corresponding encoding delays τ_j do not necessarily resemble the pattern itself [Figs. 2(b) and 2(d)].

Coupling-induced firing patterns.—We show that various firing patterns can equivalently be induced in neural networks by varying synaptic weights. To illustrate this, we first consider the Stuart-Landau LC oscillators

$$\dot{z}_j(t) = (\alpha + i\beta - |z_j(t)|^2) z_j(t) + K_j z_{j+1}(t - \tau), \quad (2)$$

where z_j are complex amplitudes and α, β are internal parameters. The phase-shift symmetry of the system allows us to look for solutions of (2) in the form $z_j(t) = \rho_j e^{i\omega t + i\varphi_j}$ with constant amplitudes ρ_j and phase shifts φ_j. Substituting this ansatz into (2), we obtain the coupling weights K_j for a given phase pattern $\{\varphi_j\}_{j=1}^N$,

$$K_j = \frac{\rho_j}{\rho_{j+1}} \frac{\omega - \beta}{\sin(\varphi_{j+1} - \varphi_j - \omega\tau)}, \quad (3)$$

where $\rho_j = \sqrt{\alpha + (\omega - \beta)\cot(\varphi_{j+1} - \varphi_j - \omega\tau)}$ are the corresponding amplitudes. Hence, for a given phase pattern $\{\varphi_j\}$ and frequency ω, one can uniquely find coupling weights $\{K_j\}$ from Eq. (3) to generate such a spatiotemporal pattern in ensemble (2). Since the stability of the predicted pattern is not known *a priori*, it is reasonable to choose ω as the frequency of a stable reference pattern in a corresponding homogeneous system with identical couplings K. In this case, $\omega - \beta = K \sin(\Delta\psi - \omega\tau)$, where $\Delta\psi = 2\pi k/N$ is a uniform phase shift of the reference traveling wave (which has to be taken into account when designing the phase pattern $\{\varphi_j\}$), and the coupling weights from Eq. (3) will lead to a stable pattern, at least for small modulations of the reference pattern.

Figure 3(a) shows an example of an S-shaped pattern in the ring of LC oscillators (2) obtained by the modulation

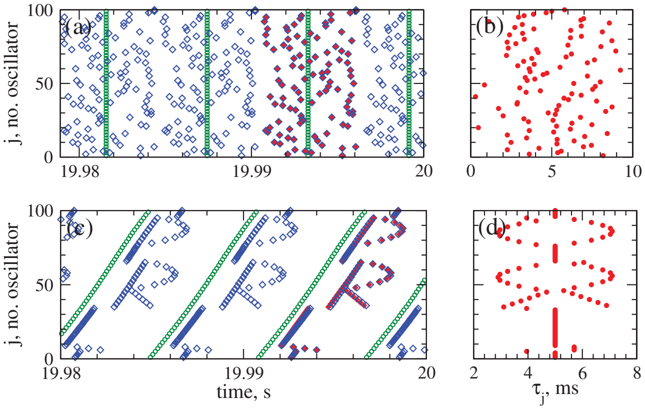

FIG. 2 (color). Examples of delay-induced spatiotemporal patterns in the HH ensemble (1). (a),(c) Raster plots of the neural firing induced by delays τ_j depicted in (b) and (d), respectively. Green circles show the corresponding reference pattern of (a) in-phase synchronization and (c) traveling wave with $k = -1$ firing fronts for identical delays $\tau_j = 5$ ms. Blue empty diamonds indicate spike onsets from numerical simulations, and red filled diamonds depict theoretically predicted patterns. To observe the above complex patterns the reference patterns were numerically continued by slowly approaching the predicted delays. Other parameters as in Fig. 1.

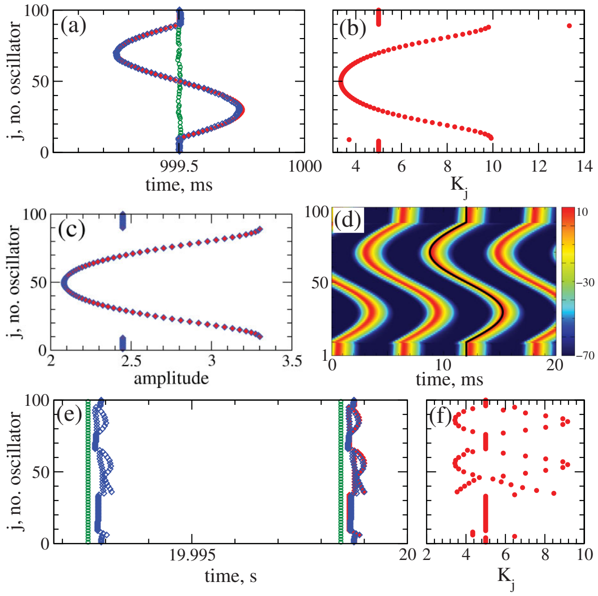

FIG. 3 (color). Examples of the coupling-induced spatiotemporal patterns of the LC (2) and HH (1) system. (a) S-shaped pattern in LC system induced by the coupling strengths K_j from (b). (c) The corresponding amplitudes ρ_j of LC oscillators. (d) Similar S-shaped pattern in the HH ensemble with the same coupling strengths. The membrane potential V_j is encoded in color. (e) Stable "PRL" pattern induced in the HH ensemble by the inhomogeneous synaptic weights K_j from (f). The weights are obtained from Eq. (3) when ignoring the amplitudes. Green circles in (a) and (e) indicate the in-phase synchronized reference pattern for homogeneous couplings $K_j = 5$. The theoretically predicted patterns [black curve in (d) and red filled diamonds in plots (a), (c), and (e)] fit well to the numerical simulations [(d) and blue empty diamonds in (a), (c), and (e)]. In (d) and (e) the theoretically predicted patterns are scaled by a factor of 13 to fit to the temporal scale of the firing pattern obtained in the HH ensemble. Parameters: $\alpha = 1$ and $\beta = \beta_j$ are Gaussian distributed with mean 1 and standard deviation 0.01. Delay $\tau_j = 5$ ms and the other parameters as in Fig. 1.

of the in-phase synchronized reference pattern oscillating at the frequency $\omega \approx 1.25\ \text{ms}^{-1}$. The coupling weights are calculated by Eq. (3) [Fig. 3(b)]. The distribution of the coupling weights significantly affects the amplitudes ρ_j of oscillators [Fig. 3(c)] as predicted above. From Eq. (3) it follows that arbitrary phase patterns are allowed with only a few exceptions: The amplitudes ρ_j (the expression under the square root) and coupling strengths K_j have to be positive, and two neighboring oscillators cannot be synchronized with a phase shift $\varphi_{j+1} - \varphi_j = \omega\tau$ (in phase if $\tau = Tn$, $n = 0, 1, \ldots$) unless all oscillators are synchronized with the same phase shift. The latter restriction can be resolved by considering complex couplings K_j.

Surprisingly, the simple expression (3) shows a very good qualitative approximation for the necessary synaptic weights in the ensemble of HH neurons (1); see Fig. 3(d). The same S-shaped pattern is achieved in the neural population for the coupling weights derived for the LC oscillators [Fig. 3(b)]. The apparent difference is that the amplitudes of the action potentials are modulated only very weakly [Fig. 3(d)] as compared to LC oscillators [Fig. 3(c)]. Therefore, ignoring the amplitudes in Eq. (3) we can create a relatively complicated "PRL" pattern in the HH ensemble [Fig. 3(e)] by an appropriate distribution of the synaptic weights according to Eq. (3) [Fig. 3(f)]. This simple expression can thus be used empirically for more complicated systems, which do not allow a reasonable analytical treatment as in the case of LC oscillators.

For the delay-induced patterns discussed above [Fig. 2], the induced time shifts in the firing of the individual neurons are independent of the model and underlying dynamics, e.g., frequency of oscillations. On the other hand, coupling-induced patterns are based on the shifts of phases, see Eq. (3), and the observed firing times do depend on the frequency of the oscillations. To illustrate this, consider the HH ensemble (1) for large delay $\tau = 20$ ms, where three stable in-phase synchronized regimes coexist [Fig. 1(e), green squares for $k = 0$]. The neurons in-phase synchronize and fire at the frequencies $f_1 \approx 57$ Hz, $f_2 \approx 97.5$ Hz, and $f_3 \approx 145$ Hz. For a predefined zigzag pattern [Fig. 4(a), red filled diamonds], Eq. (3) yields (the amplitudes being ignored) the corresponding synaptic weights $\{K_j\}$ for $\omega = 2\pi f_1 \approx 0.358\ \text{ms}^{-1}$ [Fig. 4(b), red diamonds]. The obtained coupling is then applied to the above three in-phase synchronized reference patterns [Fig. 4(a)]. In fact, the zigzag pattern is preserved, although it is significantly affected by the frequency of the oscillations. The pattern can change its size as well as orientation, as predicted by Eq. (3).

The communication delays and synaptic weights, if adjusted simultaneously, may also have cooperative effects on the spatiotemporal firing patterns. For example, the zigzag pattern [Fig. 4(a), blue diamonds] induced by inhomogeneous couplings [Fig. 4(b), red diamonds] for identical time delays can be compensated for by an appropriate adjustment of the delays [Fig. 4(b), black squares, upper horizontal axis] such that an in-phase synchronization is restored in the HH ensemble (1) [Fig. 4(a), black squares]. In such a way, the neurons fire pretty much synchronously despite the delay as well as synaptic weights in the network being nonidentical [Fig. 4(b)].

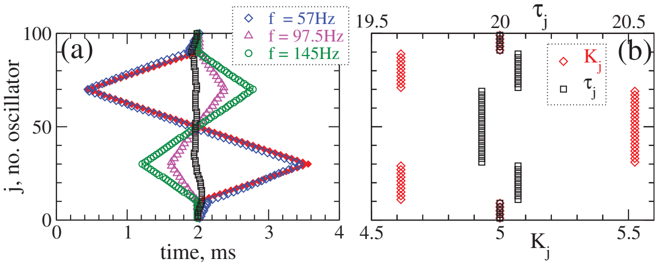

FIG. 4 (color). Impact of the oscillation frequency on the coupling-induced spatiotemporal patterns in the HH ensemble (1). (a) Zigzag patterns induced by the synaptic weights K_j [(b), red diamonds] when applied to in-phase synchronized reference patterns oscillating at different frequencies f for homogeneous coupling $K_j = 5$ and delay $\tau = 20$ ms, as indicated in the legend. The theoretically predefined pattern is depicted by filled red diamonds and scaled by a factor of 0.25. For simultaneously modified synaptic weights K_j [(b), red diamonds] and delays τ_j [(b), black squares, upper horizontal axis] the in-phase synchronization in the neural ensemble can be restored [(a), black squares]. The other parameters as in Fig. 1.

In conclusion, we showed that an arbitrary periodic spatiotemporal firing pattern can be produced by a feed-forward neural loop if communication delays or/and synaptic weights are appropriately adjusted with one restriction, namely, that each neuron fires only once per period. Since the conditions on the coupling-induced patterns are more restrictive than those on the delay-induced patterns, the adjustable delays can provide a greater encoding capacity, as expected [24]. However, the synaptic weights directly affect the phase differences between neurons, which might be important for the concept of phase delays as compared to the firing time differences explored in the auditory system [25]. A great richness of possible delay- and coupling-induced spatiotemporal firing patterns is illustrated on a minimal model of neural networks, and explicit formulas are presented which allow for a unique encoding of the patterns by communication delays and synaptic weights. The desired pattern can be addressed, e.g., either by an appropriate selection of the initial function resembling the spatial form of the pattern [see caption of Fig. 1], gradual adjustment of the coupling delays and weights starting from a reference pattern in the homogeneous network [see caption of Fig. 2], or by inducing the desired firing pattern by an external stimulation. It would also be interesting to explore how more complicated type and topology of coupling can influence the discussed patterns.

[1] B. Cessac, H. Paugam-Moisy, and T. Vieville, J. Physiol. (Paris) **104**, 5 (2009).

[2] A. K. Engel, P. König, and W. Singer, Proc. Natl. Acad. Sci. U.S.A. **88**, 9136 (1991); H. Fujii *et al.*, Neural Netw. **9**, 1303 (1996); G. Buzsaki, Neuron **68**, 362 (2010).

[3] J. J. Hopfield, Nature (London) **376**, 33 (1995); E. M. Izhikevich, Neural Comput. **18**, 245 (2006); P. Tiesinga, J. M. Fellous, and T. J. Sejnowski, Nat. Rev. Neurosci. **9**, 97 (2008); E. V. Lubenov and A. G. Siapas, Neuron **58**, 118 (2008).

[4] N. Caporale and Y. Dan, Annu. Rev. Neurosci. **31**, 25 (2008).

[5] M. Salami *et al.*, Proc. Natl. Acad. Sci. U.S.A. **100**, 6174 (2003).

[6] W. Gerstner *et al.*, Nature (London) **383**, 76 (1996); W. Senn, M. Schneider, and B. Ruf, Neural Comput. **14**, 583 (2002).

[7] C. W. Eurich *et al.*, Phys. Rev. Lett. **82**, 1594 (1999); S. Boudkkazi *et al.*, Neuron **56**, 1048 (2007); D. J. Bakkum, Z. C. Chao, and S. M. Potter, PLoS ONE **3**, e2088 (2008).

[8] A. Compston and A. Coles, Lancet **359**, 1221 (2002).

[9] T. Heil *et al.*, Phys. Rev. Lett. **86**, 795 (2001).

[10] P. Perlikowski *et al.*, Phys. Rev. E **82**, 036208 (2010).

[11] J. Zamora-Munt *et al.*, Phys. Rev. Lett. **105**, 264101 (2010); V. Flunkert *et al.*, Phys. Rev. Lett. **105**, 254101 (2010); B. B. Zhou and R. Roy, Phys. Rev. E **75**, 026205 (2007).

[12] M. Denker *et al.*, Phys. Rev. Lett. **92**, 074103 (2004); R. M. Memmesheimer and M. Timme, Physica (Amsterdam) **224D**, 182 (2006).

[13] J. G. Restrepo, E. Ott, and B. R. Hunt, Phys. Rev. Lett. **93**, 114101 (2004).

[14] C. R. Laing and A. Longtin, Physica (Amsterdam) **160D**, 149 (2001).

[15] G. E. Alexander, M. R. Delong, and P. L. Strick, Annu. Rev. Neurosci. **9**, 357 (1986).

[16] H. Bergman and G. Deuschl, Mov. Disord. **17**, S28 (2002); N. Fogelson *et al.*, Cereb. Cortex **16**, 64 (2005); C. Hammond *et al.*, Mov. Disord. **23**, 2111 (2008).

[17] M. Courtemanche, L. Glass, and J. P. Keener, Phys. Rev. Lett. **70**, 2182 (1993); R. BenYishai, D. Hansel, and H. Sompolinsky, J. Comput. Neurosci. **4**, 57 (1997).

[18] A. Hodgkin and A. F. Huxley, J. Physiol. **117**, 500 (1952) [http://jp.physoc.org/content/117/4/500]; D. Hansel, G. Mato, and C. Meunier, Europhys. Lett. **23**, 367 (1993).

[19] D. Terman, J. E. Rubin, A. C. Yew, and C. J. Wilson, J. Neurosci. **22**, 2963 (2002) [http://www.jneurosci.org/content/22/7/2963].

[20] I. Waller and R. Kapral, Phys. Rev. A **30**, 2047 (1984); F. Pasemann, Neural Netw. **8**, 421 (1995); H. Daido, Phys. Rev. Lett. **78**, 1683 (1997); P. C. Bressloff, S. Coombes, and B. de Souza, Phys. Rev. Lett. **79**, 2791 (1997); K. Pakdaman *et al.*, Phys. Rev. E **55**, 3234 (1997); I. P. Marino *et al.*, Physica (Amsterdam) **128D**, 224 (1999); S. Yanchuk and M. Wolfrum, Phys. Rev. E **77**, 026212 (2008); G. Van der Sande *et al.*, Phys. Rev. E **77**, 055202 (2008); W. Zou and M. Zhan, SIAM J. Appl. Dyn. Syst. **8**, 1324 (2009).

[21] K. A. Montgomery and M. Silber, Nonlinearity **17**, 2225 (2004); C. M. Postlethwaite and M. Silber, Physica (Amsterdam) **236D**, 65 (2007).

[22] G. B. Ermentrout and D. Kleinfeld, Neuron **29**, 33 (2001).

[23] J. Foss *et al.*, Phys. Rev. Lett. **76**, 708 (1996).

[24] W. Maass and M. Schmitt, Inf. Comput. **153**, 26 (1999).

[25] C. Leibold and J. L. van Hemmen, Phys. Rev. Lett. **94**, 168102 (2005).